Eur Biophys J (2008) 37:213–222
DOI 10.1007/s00249-007-0218-3

ORIGINAL PAPER

Estimating the dielectric constant of the channel protein and pore

Jin Aun Ng · Taira Vora · Vikram Krishnamurthy · Shin-Ho Chung

Received: 8 June 2007 / Revised: 24 July 2007 / Accepted: 24 August 2007 / Published online: 18 September 2007

Abstract When modelling biological ion channels using Brownian dynamics (BD) or Poisson–Nernst–Planck theory, the force encountered by permeant ions is calculated by solving Poisson's equation. Two free parameters needed to solve this equation are the dielectric constant of water in the pore and the dielectric constant of the protein forming the channel. Although these values can in theory be deduced by various methods, they do not give a reliable answer when applied to channel-like geometries that contain charged particles. To determine the appropriate values of the dielectric constants, here we solve the inverse problem. Given the structure of the MthK channel, we attempt to determine the values of the protein and pore dielectric constants that minimize the discrepancies between the experimentally-determined current–voltage curve and the curve obtained from BD simulations. Two different methods have been applied to determine these values. First, we use all possible pairs of the pore dielectric constant of water, ranging from 20 to 80 in steps of 10, and the protein dielectric constant of 2–10 in steps of 2, and compare the simulated results with the experimental values. We find that the best agreement is obtained with experiment when a protein dielectric constant of 2 and a pore water dielectric constant of 60 is used. Second, we employ a learning-based stochastic optimization algorithm to pick out the optimum combination of the two dielectric constants. From the algorithm we obtain an optimum value of 2 for the protein dielectric constant and 64 for the pore dielectric constant.

Keywords Dielectric constant · Brownian dynamics · MthK channel · Conductance · Ion permeation

J. A. Ng · T. Vora (✉) · S.-H. Chung
Research School of Biological Sciences,
Australian National University, Canberra, Australia
e-mail: taira.vora@anu.edu.au

V. Krishnamurthy
Department of Electrical Engineering,
University of British Columbia, Vancouver, Canada

Introduction

In Brownian dynamics (BD) simulation of biological ion channels, the trajectory of individual water molecules are not explicitly simulated. Instead, water is modelled implicitly by the net effects of incessant collisions between the ions and water molecules. These effects are represented as frictional and random forces on the ions and the dynamics of the ions are modelled by Langevin's equation. The electrostatic force acting on every ion in the simulation assembly is computed by solving Poisson's equation. Two parameters needed to solve Poisson's equation are the effective dielectric constant of water, ε_w, within the narrow pore, and of the protein, ε_p, that forms the transmembrane conduit. It is not entirely clear what values of ε_p and ε_w should be used in continuum studies of biological ion channels. The dielectric constant is a physical quantity that is hard to measure experimentally, with very few studies known to date (Gutman et al. 1992), and the complicated geometries and composition of the proteins makes this value difficult to compute analytically. Working with spatial gradients of water molecules inside the pore is a difficult problem.

Several studies have been conducted on the effective dielectric constant of proteins surrounded by water (Schutz and Warshel 2001), and the effect this has on the

surface groups and the core of the protein (Sham et al. 1997; Muegge et al. 1997; Warshel et al. 1997). On the outside of the protein, the charges are shielded by water molecules, resulting in a larger effective dielectric constant (Rees 1980; Warshel and Russell 1984; Svensson and Jönsson 1995), but the effect of charges buried deep inside the protein still remains unclear. It is hypothesized that the charges must reorient themselves, thereby increasing the effective dielectric constant (Warshel and Russell 1984; Warshel et al. 1984; Alden et al. 1995; Hwang and Warshel 1998) in the core. Simonson et al. (Simonson and Perahia 1995a, b) have used analysis of equilibrium fluctuations in the total dipole of the system to show that ε_p might vary between 2–3 inside the protein, and be as high as 10–20 at its surface. It is also likely that water closely approaches cavities in the pore to alter the surrounding protein dielectric value from its value further away from the pore. For this reason, it would be desirable to use a simulation method where the dielectric constant at the protein-water interface is an intermediate value. A further description of this is presented in the "Discussion" section.

Obviously, the rotational and translational motion of the water molecules inside the narrow channel pores will be different to that of bulk water. This constricted motion of the water molecules is caused by the charges within the protein, applied electric field and ions within the channel (Partenskii and Jordan 1992). Molecular dynamics studies of water confined in narrow pores have shown that the boundary imposes an order on the water molecules, so reducing their polarizability significantly (Green and Lu 1997; Tieleman and Berendsen 1998; Allen et al. 1999). Thus, it appears that one should use low values of ε_w in solving Poisson's equation. But precisely how low this value should be is unknown. A number of attempts have been made to determine the dielectric constant of liquid water (Neumann 1986; Alper and Levy 1989; Simonson 1996) and water inside an artificial narrow pore (Sansom et al. 1997a, b). In the latter studies mentioned above, Sansom et al. determine the dielectric constant inside the narrow artificial pores to be much lower than bulk water, with values closer to $\varepsilon_w = 30$–40.

The role of the dielectric constant ε_w in this context is simply to reduce the field inside of the ion conducting pathway by $1/\varepsilon_w$. Thus, in choosing an effective ε_w value, one has to consider by how much the screening of an ion's field is reduced in a channel compared to the bulk environment. As long as the first hydration shell of the ion remains intact in a channel, use of continuum electrostatics with ε_p closer to the bulk value may be justified. This criterion is generally satisfied in biological ion channels, including the narrow selectivity filter regions where protein atoms substitute for water, completing the solvation shell. In the case of most potassium channels, the first hydration shell is substituted by the oxygen atoms lining the selectivity filter. Using this line of reasoning, nearly all previous studies on ion channels using continuum theories adopted a high value of the pore dielectric constant, usually 60 or 80, and a value of 2 for the protein dielectric constant (Vora et al. 2006; Miedema et al. 2006).

To extract appropriate effective ε_w values that can be adopted into BD simulations and Poisson–Nernst–Planck theory, in this paper we solve an inverse estimation problem. That is, given the three-dimensional atomic model of an ion channel, we directly estimate the values of the effective ε_w and ε_p that minimize the mean square error between the simulated current obtained from BD simulations and the observed experimental current. The correct choice of the ε values to solve Poisson's equation will yield the correct profile of force encountered by permeating ions, which in turn will reproduce the experimentally determined currents flowing across the channel under various conditions. We use the MthK potassium channel model to trial number of different values of the dielectric constants and attempt to determine a dielectric constant inside the protein, ε_p, and the water-filled ion channel pore, ε_w. We note here that the values the effective dielectric constants we estimate by solving an inverse problem have no general physical significance; they may be construed as the optimal parameters which, when incorporated into BD simulations, faithfully replicate the macroscopic observables.

The MthK potassium channel is a ligand gated tetrameric cation channel. Each subunit in its transmembrane section is composed of two helices with 80 residues and a single RCK binding domain. It is an ideal candidate for these simulations. The channel was recently crystallized in its open state, with minimum coordinate manipulation, other than a slight widening of the selectivity filter region, required to obtain a conducting pore. This meant that using BD simulations could determine the conductance properties of the channel along with effective protein and pore dielectric constants. We find that the BD simulations on the crystal structure agrees well with data recently published by Li et al. (2002), in the presence of no calcium.

We show that the use of the pore dielectric constant of $\sim$60 for calculating the force acting on permeant ions accurately reproduce the experimentally-determined current–voltage relation of the MthK channel with BD. The simulated results deviate from the experimental results progressively as the value of the pore dielectric constant is lowered. In contrast, changing the value of protein dielectric constant from 2 to 10 has only a small effect on the conductance derived from BD.

Methods

Model MthK channel

The recently crystallized MthK channel (Jiang et al. 2002), at a resolution of 3.3 Å, is used to determine the effective dielectric constants of the protein and ion channel pore. The channel coordinates are initially obtained from the Protein Data Bank (PDB accession code 1LNQ). This initial structure consists of two membrane spanning helices, and a single C-terminal RCK domain on the intracellular side of each of its four subunits. The MthK channel transmembrane regions stretch from residues 19–98, followed by 17 missing residues that connect the transmembrane region to the RCK domains. To model only the transmembrane section of this protein, residues numbered 116–336 in all four subunits are removed, obtaining a pore similar to that of the KcsA channel (Doyle et al. 1998). For simulation results described here, only the transmembrane section of the MthK channel protein has been used.

Figure 1a shows a three-dimensional, cylindrically symmetric pore that is traced from the crystal structure coordinates. The channel is first aligned so that the z-axis passes through the channel pore. We then use the van der Waals radius of the pore lining atoms to trace the boundary separating the protein and the water-filled pore. This water-protein boundary is determined by measuring the minimum radius of the pore for each z value and then rotating it by 360°. In our simulations, the atoms lining the pore and forming the channel are placed at their fixed positions. Recently, Chung and Corry (2007) introduced a method of incorporating the motion of charged atoms lining the pore into BD simulations of ion conduction. Using the KcsA potassium channel, they showed that movement of the pore-lining carbonyl atoms in the selectivity filter does not severely affect the current magnitude through the channel.

The selectivity filter formed from the atomic coordinates of the MthK channel provided by Jiang et al. (2002) is not wide enough to conduct a potassium ion. For this reason, we use CHARMM (Brooks et al. 1983) to widen the filter. We apply three different harmonic forces to widen the selectivity region. These are: 60 kcal/mol/Å, decreasing to zero at r = 3.5 Å, between $15 > z > -2$ Å; 50 kcal/mol/Å, decreasing to zero at r = 5 Å, between $-3 > z > -15$ Å; and 60 kcal/mol/Å, decreasing to zero at r = 5 Å on residue 41. Initially, 300 steps of minimisation are performed using the ABNR method. Then, in order to reduce stresses within the system, the constraints are reset to the new atom positions with a weak harmonic force constant of 1 kcal/mol/Å, and the energy of the system further minimised for 100 steps. The intracellular section of the protein remains unchanged. In Fig. 1b, we show the boundary of the channel after the radius of the selectivity filter is expanded.

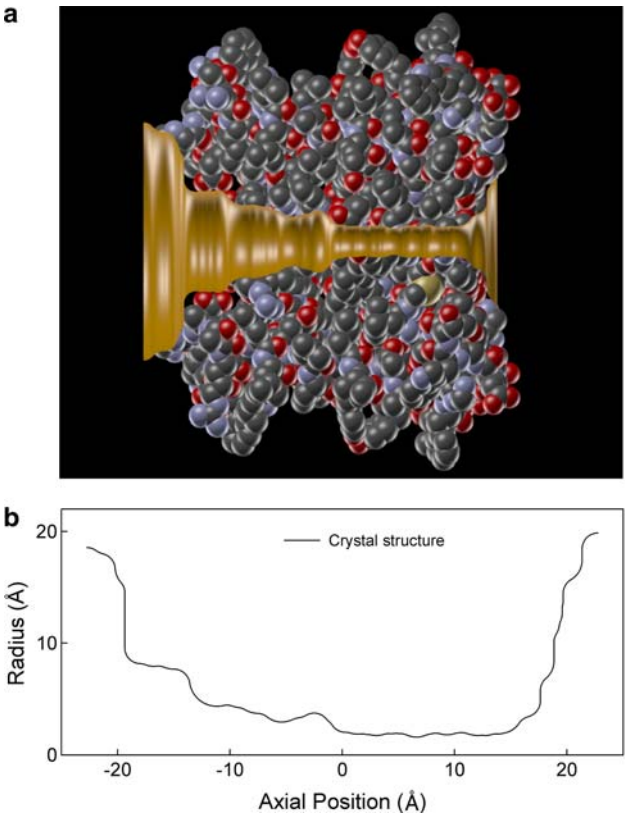

Fig. 1 Model of the MthK potassium channel. **a** Two of the four subunits of the full experimentally determined protein is illustrated. The water–protein interface is shown in gold, with the z-axis passing through the pore. The pore boundary is traced out using the minimum pore radius at each z value and then rotated around by 360°. **b** A crystal structure boundary was produced for the process of BD. This was generated from the crystal structure coordinates (Jiang et al. 2002)

Brownian dynamics model

The full atomic model of the channel, moulded from the crystal structure according to the procedures detailed above, are attached with two large reservoirs, 30 Å in radius, at each end, mimicking the intracellular and extracellular solutions. The reservoirs are filled with a fixed number of K and Cl ions, and BD simulations are performed on the channel models, by solving the following Langevin equation:

$$m_i \frac{\mathrm{d}v_i}{\mathrm{d}t} = -m_i \gamma_i v_i + \mathrm{F}_{\mathrm{R}_i} + q_i \mathrm{E}_i + \mathrm{F}_{\mathrm{S}_i}. \quad (1)$$

Here, m_i, v_i, m_i γ_i and q_i are the mass, velocity, friction coefficient and charge on an ion with index i, while $\mathrm{F}_{\mathrm{R}_i}, \mathrm{E}_i,$ and $\mathrm{F}_{\mathrm{S}_i}$ are the random stochastic force, systematic electric field, and short range forces experienced by the ion, respectively. The first term, $m_i \gamma_i \mathrm{v}_i$ is the frictional force experienced by an ion moving through a fluid. The second term, $\mathrm{F}_{\mathrm{R}_i}$, represents the random force term, arising from

the collisions between the ion and the water molecules. In our simulations, the water molecules are not treated individually, and instead are assigned a dielectric constant ε_w. The third term in Eq. 1, q_iE_i, is the electrical force and is described in detail below. The final term, F_{S_i}, is the short-range force, which arises from the close interactions of ions with each other and with the ion channel protein.

The electric force term, q_iE_i, is a result of Coulomb interactions between ions, fixed charges in the protein and image forces arising from the dielectric treatment of the water and protein regions. These are computed by solving the following partial differential equation called Poisson's equation:

$$\varepsilon_0 \nabla[\varepsilon(\mathbf{r})\nabla\phi(\mathbf{r})] = -\rho(\mathbf{r}) \tag{2}$$

in which $\varepsilon(\mathbf{r})$, $\phi(\mathbf{r})$ and $\rho(\mathbf{r})$ are the space dependent dielectric constant, electric potential and charge density, respectively. Poisson's equation is solved using the 'boundary element' method, described in detail by Hoyles et al. (1996) and Levitt (1978). To avoid solving Poisson's equation at every step of the BD simulations, the equation is solved for 0, 1 and 2 ions, at various grid positions, and stored in lookup tables (Hoyles et al. 1998). These are used during simulations, to interpolate values between grid points.

For the purpose of BD simulations, all atoms are assigned their partial charges, obtained from the CHARMM parameter set, and treated as point charges surrounded by a protein dielectric constant, ε_p. Dielectric constants of ε_p = 2, 4, 6, 8 and 10, and ε_w = 20, 30, 40, 50, 60, 70 and 80 are assigned to the protein and water, respectively, and lookup tables are constructed. As the ion moves from the bulk water-filled region of the reservoir to the narrow pore, we would expect the value of ε_w to reduce. However, performing these calculations using the boundary element method is very complicated for a sharp change in the boundary. The ideal method for implementing this change in dielectric is to introduce a switching function at the boundary. The implementation of a space dependent ε is complicated, suffering from instabilities as ions cross these boundaries. For this reason, in our implementation of different dielectric constants, we have used the same value of ε_w inside and outside the channel, and erected a Born energy barrier at the entrance and exit of the pore. This value is calculated using the Born energy equation:

$$E_B = \frac{z^2e^2N}{8\pi\varepsilon_0 r}\left(\frac{1}{\varepsilon_2} - \frac{1}{\varepsilon_1}\right) \tag{3}$$

where z, e and r denote the valence, charge and Born radius of the ion, respectively, and N is Avagadro's number. To avoid the sharp energy barriers that might arise in the BD simulations we use a smooth switching function,

$$U_B(s) = (E_B/16)\left(3s^5 - 10s^3 + 15s\right) + (E_B/2), \quad s = \frac{z - z_c}{\Delta z} \tag{4}$$

which has continuous first and second derivatives and rises smoothly from 0 to U_B as s changes from –1 to 1. For all the channel models used in this paper, the Born energy barrier is introduced, starting at the channel entrance (±18 Å) and extending 3 Å into the pore along the channel axis.

The K and Cl ions in the reservoirs are assigned random positions and velocities, and their motion is governed by the Langevin equation. Their physical properties are listed below. For the case of all simulations, symmetric solutions of 150 mM KCl was used, with 15 pairs of K and Cl ions in each reservoir. The algorithm to calculate the trajectories of the ions was devised by van Gunsteren and Berendsen (1982) and van Gunsteren et al. (1982). The velocities in the reservoirs are calculated at 100 fs time-steps, but inside the channel, where the detailed movement of the ions is important, a shorter time-step of 2 fs is used. The current for each data point is calculated by counting the number of ions crossing the channel in a fixed time. For a more detailed description of the BD implementation, we refer the reader to Corry et al. (2001), Chung et al. (1998a, b).

The masses, diffusion coefficients and ionic radii used are: for K^+, 6.5×10^{-26} kg, 1.96×10^{-9} m^2 s^{-1}, 1.33 Å; and for Cl^-, 5.9 $^{\times}$ 10^{-26} kg, 2.03×10^{-9} m^2 s^{-1}, 1.81 Å.

Adaptive controlled Brownian dynamics

We have also used an adaptive stochastic optimization (search) algorithm to efficiently estimate the optimal dielectric constant inside the MthK channel pore. This method has been used earlier, by Krishnamurthy et al. (2007), to estimate the optimal shape of a sodium channel given a finite set of possible shapes. We consider the set of 30 possible dielectric values denoted as

$$\Theta = \underbrace{\{30, 40, 50, 60, 70, 80\}}_{\varepsilon_w} \times \underbrace{\{2, 4, 6, 8, 10\}}_{\varepsilon_p}.$$

Each element of the above set Θ, is composed of one choice of water dielectric constant of the pore, ε_w, and a dielectric constant of the protein ε_p. Our aim is to compute the optimal estimate of the dielectrics, denoted θ^*, from this set Θ, to minimize the mean square error between the BD simulated current and the experimental current over a variety of experimental conditions. Mathematically:

$$\theta^* = \arg\min_{\theta\in\Theta} C(\theta), \quad \text{where } C(\theta) = \mathbf{E}\{C_n(\theta)\},$$
$$C_n(\theta) = \sum_{\lambda\in\Lambda}\left(\hat{I}_n^{(\lambda)}(\theta) - I^{(\lambda)}(\theta)\right)^2. \tag{5}$$

Here **E** denotes mathematical expectation, and

$$\lambda \in \{-160, -120, -100, -80, -40, 0, 40, 80, 100, 120, 160\}\text{mV}$$

denote the 11 different applied external potentials applied to the channel. $\hat{I}^{(\lambda)}$ denotes the BD simulated current for external potential λ (obtained using the approach described above) and $I^{(\lambda)}$ is the experimentally measured current. Since the BD simulations are conducted over batches, it is convenient to use the notation $n = 1, 2, \ldots$ to denote the batch number. The various experimental conditions are denoted by $\lambda \in \Lambda$, which in this case are the various applied potentials used earlier to construct the current–voltage curve. Thus, $C_n(\theta)$ is the minimization between the BD simulated current, $\hat{I}$, and the experimental current I, at a particular applied potential λ, for a particular run number n.

The implementation of the stochastic optimization algorithm to estimate the optimal dielectric pair θ^* in Eq. (5) is described below: At a batch-time $n = 0$, a set of dielectric constants ε_w and ε_p, represented by the state θ is randomly selected from the set of possible combinations with uniform probability. This is the initial estimate of the optimal dielectric constants ε_w and ε_p. A set of independent simulations on all experimental conditions λ is performed and $C_n(\theta)$ is calculated. We then generate an alternative candidate $\tilde{\theta}_n$ and conduct Λ independent simulations on the new candidate $\tilde{\theta}_n$ and evaluate $C_n(\tilde{\theta}_n)$. These two values are then compared, so that the candidate with the better estimate of the dielectric constants moves to the next simulation step $n + 1$, as the optimal candidate, and a new second candidate is selected. After a number of steps the algorithm is seen to converge at a particular choice of ε_w an dε_p. It is also seen to spend more time at the optimal candidate θ^* than at any other candidate θ. Further details of the algorithm and extensions can be found in Krishnamurthy et al. (2007). The attraction capability of this algorithm is proved by Andradottir (1999).

Results

To determine the effects of varying dielectric constants on the energetics of ion permeation, we first construct electrostatic energy profiles by passing a single K^+ ion through the channel. The K^+ ion is moved at 1 Å intervals through the central axis of the pore, and Poisson's equation is solved to calculate the energy landscape encountered by the ion.

The profiles displayed in Fig. 2a reveal the effects of increasing ε_w from 20 to 80 in steps of 10. For this calculation, ε_p is kept constant at 2. We see that when a K^+ ion is moved through the channel, for different dielectric constants of the water-filled pore, the depth of the energy well within the channel decreases progressively as the dielectric constant ε_w. The maximum depth of the energy well at z = 15 Å changes from 44 kT for ε_w = 20 to 20 kT for ε_w = 80. This is a result of the increased repulsive image forces experienced by the incoming ion from the surrounding protein walls. Fig. 2b shows a similar energy profile created for a K^+ ion moving through the z-axis of the channel with varying protein dielectric constants, ranging from ε_p = 2 to ε_p = 10. The depth of the energy well is progressively reduced when ε_p is reduced.

BD simulations are performed on the MthK channel model to collect current–voltage data. There are two sets of experimentally-determined current–voltage curves for the MthK channel. The curve reported by Jiang et al.

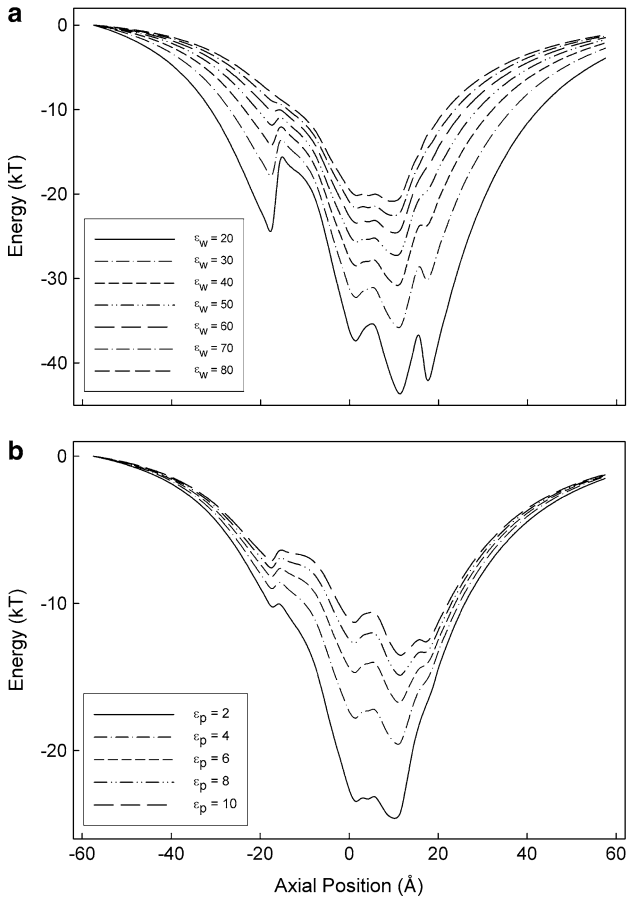

Fig. 2 Potential energy profiles of a single potassium ion are calculated at an applied potential of 0 mV. Poisson's equation is solved as the permeating ion is moved at 1 Å steps along the channel axis and its potential energy calculated. All profiles are shown for the crystal structure with **a** ε_w = 20,30,40,50,60,70,80 and ε_p = 2, and **b** ε_w = 60 and ε_p = 2,4,6,8,10

(Jiang et al. 2002) shows a pronounced inward rectification; the currents at +150 and –150 mV are, respectively, +6 and –30 pA. It is found experimentally, that when calcium ions are removed from the intracellular side, the outward current increases, and the relationship can be closely approximated with a linear curve (Li et al. 2002). For our present study, all our simulations are performed with no calcium ions in the assembly, and our results are compared with the experimental measurements obtained by Li et al. (2002).

The crystal structure is selected for the construction of a set of current–voltage curves with different protein and water dielectric constants. Simulations are first performed on the channel model with pore dielectric constants of ε_w = 20, 30, 40, 50, 60, 70, and 80 under various values of the driving potential. For these simulations, we assign a value of ε_p = 2 as the dielectric constant of the protein. The curves obtained from BD simulations are displayed in Fig. 3. The dielectric constants of ε_w = 60 (Fig. 3a, filled circles) and 70 (Fig. 3b filled triangles), both provide good agreement with experimental results.

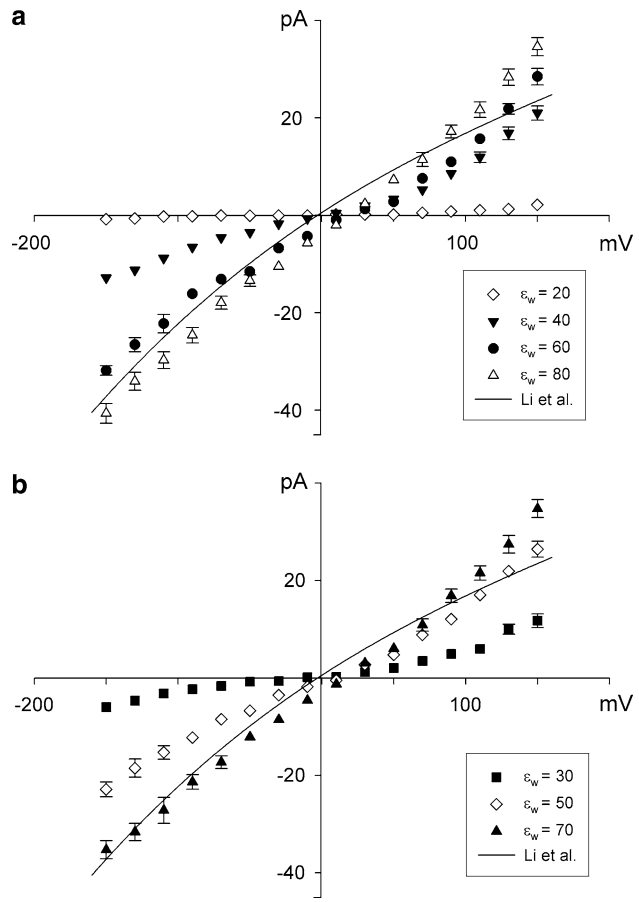

Fig. 3 Current–voltage curves with varying ε_w. Simulations were performed with 150 mM KCl in each reservoir. A dielectric constant of ε_p = 2 was used for the protein. **a** Plots of ε_w = 20,40,60,80 and **b** ε_w = 30, 50, 70. Experimental curves by Li et al. (2002) (*solid line*) with no calcium in the internal solution, are also plotted for comparison. In this and the following figures, a data point represent the average of 10–20 sets of simulations, each set lasting 2×10^6 time-steps (or 0.2 μs). *Error bars* in this and following figures have a length of 2 SEM and are not shown when they are smaller than the data points

The crystal structure is also used to determine the optimum value for the protein dielectric constant. For these simulations, the water in the pore is assigned a dielectric constant of ε_w = 60, while the protein is assigned dielectric constants of ε_p = 2, 4, 6, 8 and 10. A current–voltage curve is constructed for each set of dielectric constants, the values of which are plotted in Fig. 4. In agreement with an earlier study (Chung et al. 2002), we find that changing the dielectric constant of the protein does not have an acute effect on the current through the channel. However, the value of ε_p = 2 has the closest fit to the data, as determined from the square of differences between the experimental and simulated measurements.

The current–voltage curves displayed in Fig. 3 are obtained by setting ε_p constant at 2 and then varying ε_w from 20 to 80 in steps of 10. Similarly, those shown in Fig. 4 are obtained by using a fixed value ε_w = 60 and varying ε_p from 2 to 10 in steps of 2. Using adaptive controlled BD, we test all possible combinations of ε_w = 30, 40, 50, 60, 70, 80 and ε_p = 2, 4, 6, 8, 10. This learning-based, dynamic stochastic optimization algorithm picks out a pair of the two dielectric constants, ε_p and ε_w, for which the mean square error between the BD simulated current and the actual observed experimental current is the minimum. The key idea behind this approximation algorithm is to make comparisons between two possible dielectric constants, say ε_w = 60 and ε_p = 2 with ε_w = 40 and ε_p = 6, and compute the mean square errors. The algorithm runs more BD simulations for the pairs that yield closer approximation to the measured

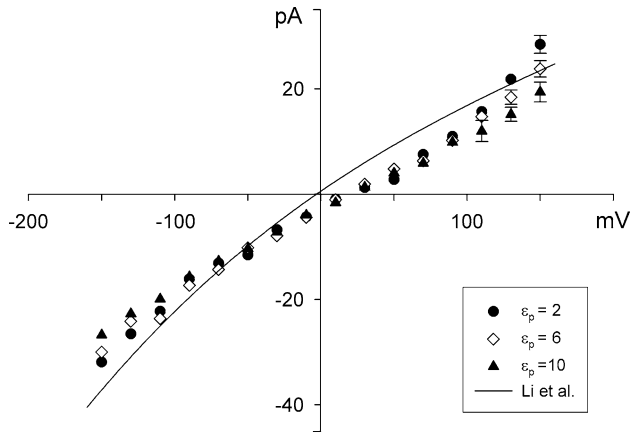

Fig. 4 Current–voltage curves with varying ε_p. Simulations were performed with 150 mM KCl in each reservoir. A dielectric constant of ε_p = 60 was used for the protein. ε_p = 2, 4, 6, 8, 10 were used for the protein, however, only ε_p = 2, 6, 10 are shown. Experimental curves by Li et al. (2002) (*solid line*) with no calcium in the internal solution, are also plotted for comparison

currents and spends less time computing the current for other pairs. Thus, the optimum pair is selected most frequently for making pairwise comparisons. Figure 5a shows the number of times each pair of the protein and water dielectric constants is selected for testing. The largest peak is observed for $\varepsilon_w = 60$ and $\varepsilon_p = 2$. We run a similar series of tests with finer steps of ε_w. The values of ε_w we use for this series range from 50 to 70, in steps of 2, and of ε_p from 2 to 10 in steps of 2. In Fig. 5b, we plot the computational effort the algorithm expends, or the number of times each model is selected for testing. The peak occurs for the pair whose ε_w and ε_p values are 64 and 2, respectively. Although the current–voltage curves appear to be somewhat insensitive to the choice of ε_p (Fig. 4), the results obtained from adaptive controlled BD clearly reveal that the value of $\varepsilon_p = 2$ is the optimal choice for matching the simulated and experimental results. We calculate the average square deviations between the simulated and experimental currents, $C_n(\tilde{\theta}_n)$ at all applied potentials. The value we obtain for the case of $\varepsilon_w = 64$ and $\varepsilon_p = 2$ is 33 pA^2. The corresponding values when ε_p is changed to 4, 6, 8 and 10 are, respectively, 532, 510, 239 and 164 pA^2.

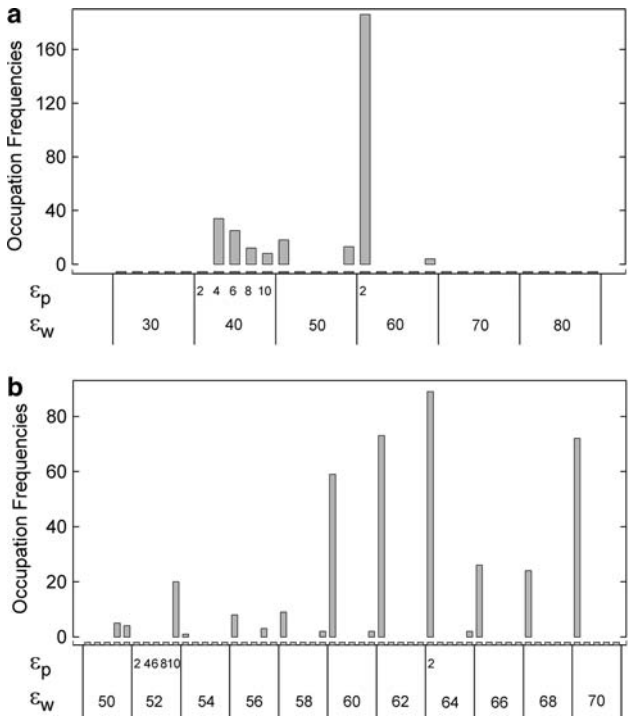

Fig. 5 The optimum combination of ε_w and ε_p determined from adaptive controlled BD simulations. **a** All possible combinations of $\varepsilon = 20$, 30, 40, 50, 60, 70 and 80 and $\varepsilon_p = 2$, 4, 6, 8 and 10 were tested pairwise. For each test, the simulated currents at the applied potentials of –160, –120, –100, –80, –40, 0, +40, +80, +100, +120 and +160 mV were compared with the experimental currents obtained at the corresponding values. The model that assumed the $\varepsilon_w = 60$ and $\varepsilon_p = 2$ was selected most often to compare with the other models that assumed different combinations of the two dielectric constants. (B) All possible combinations of $\varepsilon = 50$–70 in steps of 2 and $\varepsilon_p = 2$ to 10 in steps of 2 were tested at the applied potentials as in (A). The model with $\varepsilon_w = 64$ and $\varepsilon_p = 2$ was selected most often to compare with the other models that assumed different combinations of the two dielectric constants

Discussion

We have used BD simulations to deduce the effective dielectric constants of the MthK potassium channel protein and of the water-filled ion-conducting conduit. Several early studies on proteins have noted the protein dielectric constant, ε_p, to be as high as 10–20 on the outer surface of the protein (Simonson and Perahia 1995a, b) and the dielectric constant of the artificial water-filled channel pores, ε_w, to be as low as 30 (Sansom et al. 1997a, b). We have used a reverse engineering method to establish the most appropriate values of the dielectric constants that best fit the experimental observations by carrying out BD simulations with a number of different dielectric constant values. Using this approach, we find that $\varepsilon_p = 2$ and $\varepsilon_w = 60$, when used in solving Poisson's equation, replicate the experimental results most closely.

In addition to the effective dielectric constants, one other free parameter features in the calculation of currents flowing across the model channel using a continuum theory, namely the diffusion coefficient of each ion species in the simulation assembly. With the Poisson–Nernst–Planck theory, a fortuitous match between experimentally determined current–voltage relationships and those calculated theoretically is obtained by adjusting this parameter (Nonner and Eisenberg 1998; Chen et al. 1999). Currents measured using this theory scale linearly with the value of assumed diffusion coefficient. In BD, altering the diffusion coefficients has no significant effect on channel currents. Chung et al. (1998a) systematically examined the influence of diffusion coefficient on conductance. In contrast to bulk conductance, where current is proportional to the diffusion coefficient, the current in the potassium channel decreases at a very slow rate until the diffusion coefficient is reduced to 1/3 or 1/4 of the bulk value. In this study, as in all our previous studies using BD, we adopted the values of ionic diffusion coefficients determined from molecular dynamics studies (Allen et al. 1999).

We use an average value of the dielectric constant throughout the protein, and thus, do not consider localised effects. This might explain a lower value than those found in other theoretical studies. However, since we do not experience a significant change in current through the pore with increasing dielectric constant, ε_p, we believe that the dielectric constant of the protein must lie somewhere between 2 and 10, but the charged amino acid groups comprising the channel are what play a central role in the conduction mechanism.

The molecular dynamics studies used to calculate the dielectric constant of water in artificial pores are not without limitations. In the previous studies (Sansom et al. 1997a, b), extremely high applied voltages of 600 mV to up to 2 V are used across the membrane, which may cause the dielectric to break down (Freeman et al. 1994). Realistic potentials are only up to a couple of hundred millivolts across the membrane. Also, the authors themselves agree that the neglect of long-range forces can cause a lower estimation of the dielectric constant of water in the pore. It is possible that in certain regions of the channel, such as the selectivity filter, the dielectric constant of water might be lower, due to the single filing of the water molecules seen in molecular dynamics studies. However, we expect in the wider regions such as the intracellular vestibule, the dielectric constant would be considerably higher. Of course, its value depends highly on the geometry of the channel, the electric field generated by the charged residues within the protein, and the external applied electric field.

It is possible to divide the protein into several layers, and assign a high value of the dielectric constant for the layer bordering the water-protein interface and gradually decrease ε_p values to a low value of 2 for the interior layer, as proposed by Simonson and Perahia (1995a). They suggest that the surface charge groups could be treated as part of the solvent, or as another intermediate dielectric region. Similarly, we can use multiple regions of varying dielectric constants along the ion-conducting pathway. This would allow us to assign a lower dielectric constant in the selectivity filter, where the water molecules are in single file, and a larger dielectric constant region in the intracellular vestibule. Such a refinement and extension of the current attempt, making use of finite difference method in solving Poisson's equation, will be the subject of our future study. Our current study, despite the simplifications, clearly reveal that one can select an average value ε_p of the entire channel protein and an average value ε_w of the water inside of the MthK channel pore which reliably replicate the experimental current–voltage relationships.

There is one important advantage in using the MthK potassium channel to deduce the effective dielectric constants. Unlike many other channels whose atomic coordinates are available, we note that the MthK channel requires minimal structural modifications to construct a functioning pore. Once the RCK domain is removed and the selectivity filter is slightly expanded such that its radius equals that of potassium, the MthK channel selectively conducts K^+ ions when it is incorporated into BD. To render the KcsA channel permeable to cations, the structure of the intracellular gate needs to be manipulated and some of the ionized residues, such as the E51–R52 and E71–R27 pairs and R27 residue, have to be neutralized (Chung et al. 2002). No such adjustments are needed for the MthK channel. Also, a recent report by Jiang et al. (2002) reveals that the degree of inward rectification observed in this channel is dependent on the presence of Ca^{2+} ions in the intracellular side of the membrane. Such Ca^{2+}-dependent attenuation of outward currents has been shown for the Na^+ channel (Vora et al. 2006; French et al. 1994). It is generally seen that there is better agreement with the inward experimental curve, at higher values of dielectric constants, than the outward current. We hypothesize that this is possibly related to the gating mechanism of the channel, that is driven by calcium ions. Since we do not incorporate calcium ions in our simulations, and have removed the RCK domains, it is difficult to make any conclusive statements regarding this phenomenon. However, we do find that our simulation results agree well with the no-calcium data by Li et al. (2002).

In general, conclusions drawn and inferences made from electrostatics are not valid in regions that are small compared to the diameter of water molecules or an ion. In the constricted region of the channel, such as the selectivity filter of potassium channels, the radius of the pore is about the same as that of potassium. Also, in such regions water molecules are ordered (Sansom et al. 1997) and are not free to align with the external field. Thus, it is not clear if a uniform value of the dielectric constant can be assigned for water-filled conduits in biological ion channels. Our study reported here clearly demonstrates that currents determined under various experimental conditions can be faithfully reproduced by BD simulations, in which the forces acting on permeant ions are computed by solving Poisson's equation with appropriate values of the dielectric constants. Using a reverse engineering approach, we find that a water dielectric constant of 64 in the water-filled pore, and a protein dielectric constant of 2 for the transmembrane channel protein, captures many of the salient properties of potassium channels.

Acknowledgments This work was supported by grants from the National Health & Medical Research Council of Australia. Calculations were performed on the SGI Altix cluster at the APAC National Facility.

Appendix

The algorithm for the adaptive controlled BD simulations is presented here:

Algorithm 1: Stochastic Search Adaptive BD Algorithm for Dielectric Estimation

- `Step 0`: (Initialisation) At batch-time $n = 0$, initialise state of the algorithm by selecting a dielectric constant

θ_0, a combination of ε_w and ε_p, as the optimal dielectric estimate of ion channel pore and protein randomly and with uniform probability.

- `Step 1`: (sampling and exploration) at a particular batch n, we conduct independent simulations on all experimental conditions Λ, and evaluate $C_n(\theta_n)$ according to Eq. 5. We then generate an alternative candidate $\tilde{\theta}_n$ and conduct Λ independent simulations on the new candidate $\tilde{\theta}_n$, and evaluate $C_n(\tilde{\theta}_n)$.
- `Step 2`: (conditional acceptance test) the candidate with the lower $C_n(\theta)$ value is the better fit to the experimental results. It is the better dielectric estimate for batch n. It is then selected as the optimal candidate for run $n + 1$ and another θ (choice of ε_w and ε_p) is randomly chosen as the comparison candidate.
- `Step 3`: update π_n, which is a counter for the number of times each set of candidates has been a better estimate of the experimental results.
- `Step 4`: update estimate of ε_w and ε_p. Go to Step 1.

The function $\pi_n(\theta)$ of π_n generated in Step 3 of the above algorithm is merely a normalised counter for how many times the algorithm has visited any particular candidate of dielectric constants. In particular,

$$\pi_n(\theta) = \frac{\text{No. of times algorithm visits a particular set of } \varepsilon_w \text{ and } \varepsilon_p \text{ in batches 1 to } n}{n} \tag{6}$$

is the occupation probability of state θ. We see that for sufficiently large n, $\pi_n(\theta^*) > \pi_n(\theta)$, meaning that the algorithm spends more time at the optimal shape θ^* than at any other shape $\theta \in \Theta$. As a consequence θ_n^*, which is the optimal shape on which the algorithm has spent maximum time until time n, converges to the optimal shape θ^* with probability one. The attraction capability of this algorithm is proved by Andradottir (1999).

References

Alden RG, Parson WW, Chu ZT, Warshel A (1995) Calculations of electrostatic energies in photosynthetic reaction centers. J Am Chem Soc 117:12284–12298

Allen TW, Kuyucak S, Chung SH (1999) The effect of hydrophobic and hydrophilic channel walls on the structure and diffusion of water and ions. J Chem Phys 111:7985–7999

Alper HE, Levy RM (1989) Computer simulations of the dielectric properties of water: studies of the simple point charge and transferable intermolecular potential models. J Chem Phys 91:1242–1251

Andradottir S (1999) Accelerating the convergence of random search methods for discrete stochastic optimization. ACM Trans Model Comput Simul 9(4):349–380

Brooks BR, Bruccoleri RE, Olafson BD, States DJ, Swaminathan S, Karplus M (1983) CHARMM: a program for macromolecular energy, minimisation, and dynamics calculations. J Comp Chem 4:187–217

Chen DP, Xu L, Tripathy A, Meissner G, Eisenberg B (1999) Selectivity and permeation in calcium release channel of cardiac muslce: alkali metal ions. Biophys J 76:1346–1366

Chung SH, Corry B (2007) Conduction properties of KcsA measured using Brownian dynamics with flexible carbonyl groups in the selectivity filter. Biophys J 93:44–53

Chung SH, Allen TW, Hoyles M, Kuyucak S (1998a) Permeation of ions across the potassium channel: Brownian dynamics studies. Biophys J 77:2517–2533

Chung SH, Hoyles M, Allen TW, Kuyucak S (1998b) Study of ionic currents across a model membrane channel using Brownian dynamics. Biophys J 77:793–809

Chung SH, Allen TW, Kuyucak S (2002) Conducting-state properties of the KcsA potassium channel from molecular and Brownian dynamics simulations. Biophys J 82:628–645

Corry B, Allen TW, Kuyucak S, Chung SH (2001) Mechanisms of permeation and selectivity in calcium channels. Biophys J 80:195–214

Cox DH, Cui J, Aldrich RW (1997) Separation of gating properties from permeation and block in *mslo* large conductance Ca-activated K^+ channels. J Gen Physiol 109:633–646

Doyle DA, Cabral JM, Pfuetzner RA, Kuo A, Gulbis JM, Cohen SL, Chait BT, MacKinnon R (1998) The structure of the potassium channel: molecular basis of K^+ conduction and selectivity. Science 280:69–77

Freeman SA, Wang MA, Weaver JC (1994) Theory of electroporation of planar bilayer-membranes—prediction of the aqueous area, change in capacitance, and pore–pore separation. Biophys J 67:42–56

French RJ, Worley III JF, Wonderlin WF, Kularatna AS, Krueger BK (1994) Ion permeation, divalent ion block, and chemical modification of single sodium channels. J Gen Physiol 103:447–470

Green ME, Lu J (1997) Simulation of water in a small pore: effect of electric field and density. J Phys Chem B 101:6512–6524

Gutman M, Tsfadia Y, Masad A, Nachiel E (1992) Quantification of physical-chemical properties of the aqueous phase inside the phoE ionic channel. Biochim Biophys Acta 1109:141–148

Hoyles M, Kuyucak S, Chung SH (1996) Energy barrier presented to ions by the vestibule of the biological membrane channel. Biophys J. 70:1628–1642

Hoyles M, Kuyucak S, Chung SH (1998) Computer simulation of ion conductance in membrane channels. Phys Rev E 58:3654–3661

Hwang JK, Warshel A (1998) Why ion pair reversal by protein engineering in unlikely to succeed. Nature 334:270–273

Jiang Y, Lee A, Chen J, Cadene M, Chait BT, MacKinnon R (2002) Crystal structure and mechanism of a calcium-gated potassium channel. Nature 417:515–522

Krishnamurthy V, Vora T, Chung SH (2007) Adaptive Brownian dynamics for shape estimation of sodium ion channels. J Nanosci Nanotechnol 7:2273–2282

Levitt DG (1978) Electrostatic calculations for an ion channel: I. energy and potential profiles and interactions between ions. Biophys J 22:209–219

Li Y, Berke I, Chen L, Jiang Y (2002) Gating and inward rectifying properties of the MthK K^+ channel with and without the gating ring. J Gen Physiol 129:109–120

Miedema H, Vrouenraets M, Wierenga J, Gillespie D, Eisenberg B, Meijberg W, Nonner W (2006) Ca^{2+} selectivity of a chemically modified OmpF with reduced pore volume. Biophys J 91:4392–4400

Moczydlowski E, Latorre R (2002) Gating kinetics of Ca^{2+}-activated K^+ channels from rat muscle incorporated into planar lipid bilayers. Evidence for two voltage-dependent Ca^{2+} binding reactions. J Gen Physiol 495:701–716

Muegge I, Schweins T, Langen R, Warshel A (1997) Electrostatic control of GTP and GDP binding in the oncoprotein p21ras. Structure 4:475–489

Neumann M (1986) Dielectric relaxation in water. Computer simulations with the TIP4P potential. J Chem Phys 85:1567–1580

Nonner W, Eisenberg RS (1998) Ion permeation and glutamate residue linked by Poisson–Nernst–Planck theory in L-type calcium channels. Biophys J 75:1287–1305

Partenskii MB, Jordan PC (1992) Nonlinear dielectric behavior of water in transmembrane ion channels: ion energy barriers and the channel dielectric constant. J Phys Chem 96:3906–3910

Rees DC (1980) Experimental evaluation of the effective dielectric constant of proteins. J Mol Biol 141:323–326

Sansom MSP, Smith GR, Adcock C, Biggin PC (1997a) The dielectric properties of water within model transbilayer pores. Biophys J 73:2404–2415

Sansom MSP, Kerr ID, Breed J, Sankaramakrishnan R (1997b) Water in channel-like cavities: structure and dynamics. Biophys J 70:693–702

Schutz CN, Warshel A (2001) What are the dielectric "constants" of proteins and how to validate electrostatic models? Proteins 44: 400–417

Sham YY, Chu ZT, Warshel A (1997) Consistent calculations of pKa's of ionizable residues in proteins: semi-microscopic and microscopic approaches. J Phys Chem 101:4458–4472

Simonson T (1996) Accurate calculation of the dielectric constant of water from simulations of a microscopic droplet in vacuum. Chem Phys Lett 250:450–454

Simonson T, Perahia D (1995a) Internal and interfacial dielectric properties of cytochrome c from molecular dynamics in aqueous solution. Proc Natl Acad Sci USA 92:1082–1086

Simonson T, Perahia D (1995b) Microscopic dielectric properties of cytochrome c from molecular dynamics simulations in aqueous solution. J Am Chem Soc 117:7987–8000

Svensson B, Jönsson B (1995) An efficient simulation technique for electrostatic free energies with application to azurin. J Comp Chem 16:370–377

Tieleman DP, Berendsen HJ (1998) A molecular dynamics study of the pores formed by *Escherichia coli* OmpF porin in a fully hydrated palmitoyloleoylphosphatidylcholine bilayer. Biophys J 74:2786–2801

van Gunsteren WF, Berendsen HJC (1982) Algorithms for Brownian dynamics. Mol Phys 45:637–647

van Gunsteren WF, Berendsen HJC, Rullmann JA (1982) Stochastic dynamics for molecules with constraints: Brownian dynamics of *n*-alkanes. Mol Phys 44:69–95

Vergara C, Latorre R (2002) Kinetics of Ca^{2+}-activated K^+ channels from rabbit muscle incorporated into planar bilayers. Evidence for a Ca^{2+} and Ba^{2+} blockade. J Gen Physiol 82:543–568

Vora T, Corry B, Chung SH (2006) Brownian dynamics investigation into the conductance state of the MscS channel crystal structure. Biochim Biophys Acta Biomembranes 1668:106–116

Warshel A, Russell ST (1984) Calculations of electrostatic interactions in biological systems and in solutions. Q Rev Biol 17:283–422

Warshel A, Russell ST, Churg AK (1984) Macroscopic models fro studies of electrostatic interactions in proteins: limitations and applicability. Proc Natl Acad Sci USA 81:4785–4789

Warshel A, Papazyan A, Muegge I (1997) Microscopic and semimicroscopic redox calculations: what can and cannot be learned from continuum models. J Biol Inorg Chem 2:143–152